coasts

MDPI

Article

Geomorphological Evolution of the Andaman Sea Offshore Phang Nga Province (Thailand) during the Holocene: An Example for a Sediment Starving Shelf

Peter Feldens [1,*], Klaus Schwarzer [2], Daroonwan Sakuna-Schwartz [3] and Somkiat Khokiattiwong [4]

[1] Leibniz Institute for Baltic Sea Research Warnemünde, Marine Geology, 18119 Warnemünde, Germany
[2] Institute of Geosciences, Coastal Geology and Sedimentology, Kiel University, 24118 Kiel, Germany; klaus.schwarzer@ifg.uni-kiel.de
[3] Freithof 26, 41460 Neuss, Germany; daroonwans@gmail.com
[4] Phuket Marine Biological Center, P.O. Box 60, Phuket 83000, Thailand; skhokiattiwong@gmail.com
* Correspondence: peter.feldens@io-warnemuende.de

Abstract: Understanding the development of shallow seas is essential, as they provide a major environmental and economic resource. An investigation of the Holocene development and the present conditions of the Andaman Sea shelf was carried out based on hydroacoustic surveys and sedimentological sampling. The results show that the relative sea level in the offshore Phang Nga province (Thailand) was at a present-day water depth of approximately 63 m at 13 cal ka BP. This agrees with the sea level development of the Sunda Shelf. Since that time, the Andaman Sea continental shelf developed as a sediment-starved environment, with less than 2 m thickness of sediment deposited during the Holocene on the crystalline basement over large areas between 60 m and 20 m water depth. Between 28 and 17 m water depth, a series of moribund asymmetrical sand ridges exist. These ridges were formed around 9.0 ka cal BP. They strike oblique to the coastline. On the seaward side of the sand ridges, small NW-SE directed submarine dunefields developed, shaped by monsoon-induced currents.

Keywords: shelf evolution; sediment dynamics; sand ridges; sea level rise; acoustic backscatter

Citation: Feldens, P.; Schwarzer, K.; Sakuna-Schwartz, D.; Khokiattiwong, S. Geomorphological Evolution of the Andaman Sea Offshore Phang Nga Province (Thailand) during the Holocene: An Example for a Sediment Starving Shelf. *Coasts* **2022**, 2, 1–16. https://doi.org/10.3390/coasts2010001

Academic Editor: Philip Collins

Received: 3 December 2021
Accepted: 20 January 2022
Published: 26 January 2022

1. Introduction

Shelf seas—ranging from the coastline to the shelf break—cover ca. 8% of the marine environment, are highly productive areas of the oceans regarding biological activity and fishing resources and are exploited regarding mineral resources. They are often characterized by complex patterns of sediment distribution, geomorphological structures and sediment dynamics [1]. Tides, wave action, residual circulation and sediment gravity flow enhance the dispersal of sediments and are the major driving forces for the geomorphological and sedimentological development of coastal and shelf environments. While tidal currents generate a landward sediment transport, on the upper shelf waves disperse and sort the sediment [2], generating an onshore-directed transport of coarse-grained material while finer fractions are moved offshore. Areas with sediment deficiency and areas of sediment accumulation point to different framework conditions of hydrodynamic forces, geological prerequisites and sedimentological built up. Comparisons of these different environments provide insights into the postglacial geological evolution of a particular shelf as well as into recent sediment dynamic processes [3]. Continental shelves have experienced a series of sea level fluctuations and sedimentation processes throughout the Quaternary [4]. Generally, sediment accumulation is controlled by the rate of relative sea-level rise, the rate and character of sediment input, the geomorphological gradient of the shelf and its geological composition, the hydrodynamic driving forces and the resulting rate of sediment transport. Depending on the ratio of these parameters and the interaction

of different processes, continental shelves have evolved from diverse structural origins toward a characteristic shelf configuration [5]. Huge areas of present-day continental mid- and inner shelf regions are sediment starved [6–8] and are considered to be characterized by a high energetic hydraulic regime, reoccurring erosion and ecologically valuable hard bottom substrates [4]. Today, 60–70% of the shelf sediments are relict deposits that accumulated during the last glacial period when the sea level was lowered to approximately 120 m below the present sea level [9,10], thus exposing shelf environments to terrestrial conditions. During the initial phases of the early Holocene sea level rise, shelf sediments have been partly reworked and redistributed, leaving remnants of young Pleistocene and early Holocene deposits and drowned geomorphological and sedimentological bedforms behind [11]. In the near future, sea level rise will continue to impact shelf sediments and coastlines, with the highest accelerations observed in the Indo-Pacific and South Atlantic [12]. On shelves without strong fluvial sediment discharge of siliciclastic material such as the Andaman Sea, sediment-starving shelves develop even when new sediment is formed in situ, as in tropical environments, by carbonate production [13]. Sediment-starved shelves are typically characterized by the formation of an armor layer on the seafloor that is not eroding and transported, except during extraordinary events such as tsunamis, typhoons/hurricanes or severe storms [14]. On these shelves, unique bedforms develop, not only depending on current velocity, grain size distribution and water depth, but also on sediment availability, which plays a dominant role as well [8,15,16].

The research project TUNWAT (Tsunami deposits in nearshore and coastal waters of Thailand [14]) was set up to investigate the impact of the 2004 Indian Ocean Tsunami on the shelf environment offshore of the Thai coast of the Andaman Sea. A large amount of geoscientific information gathered in the project is not directly related to the impact of the Tsunami but provides potentially valuable information for future studies about the local geological setting, Holocene evolution, sediment transport processes, geomorphological development and human intervention on the inner Andaman Sea shelf. This contribution aims to make these data available and to provide information about the continental shelf offshore of Phang Nga Province regarding the sediment distribution and the occurrence of geomorphological structures such as sand ridges and submarine dunes on a sediment-starved shelf. In addition, findings regarding shelf development due to the Holocene sea level rise and the impact of tin mining activities on the seafloor are reported.

2. Regional Setting and Methods

2.1. Regional Setting

The Andaman Sea (Figure 1), located along the eastern side of the Indian Ocean between the Malay Peninsula and the Andaman and Nicobar Islands, is a backarc basin with a complex bottom topography [17]. The Andaman-Nicobar Ridge isolates the Andaman Sea from the Bay of Bengal. In the northern region, a submarine delta has been built by the outflow of the Ayeyarwady (Irrawaddy) and Salween rivers [18]. The delta is connected to the eastern shallow shelves along the Malay Peninsula. From the shelves, the sea bottom drops off sharply into a large central basin and two smaller basins deeper than 2000 m. While some sedimentological information on the shelf offshore of Myanmar is available [19,20], the Andaman Sea continental shelf of Thailand is poorly investigated. Some exploration activity has been carried out by the oil industry, by the tin mining industry and by the Department of Mineral Resources of Thailand [21,22], but to our knowledge these data are not accessible by the public.

The Andaman Sea continental shelf adjacent to the Malay Peninsula is narrow and slightly inclined [23]. In offshore Phang Nga province, the 50 m depth contour is reached about 30 km offshore at a distance to the shelf break of about 80 km; here, submarine mass-wasting occurs [24]. It is a wave-dominated, high energy erosional coast with only a thin cover of Quaternary deposits [25]. Monsoonal winds include the northeast monsoon, lasting from mid-October to March, and the southwest monsoon, lasting from May to September. The latter generates its highest waves along the Andaman Sea coast. Strong

winds occasionally reach gale force, while typhoons only affect the investigation area infrequently [26,27]. The micro to mesotidal regime shows a maximum tidal range of 3.6 m during spring tide [28]. N-S directed tidal currents dominate the longshore transport [25]. Sediments discharged by the Ayeyarwady River, which are highly seasonal, with more than 80% of their annual discharge occurring during the SW monsoon [19], do not reach this part of the Andaman Sea [18,20].

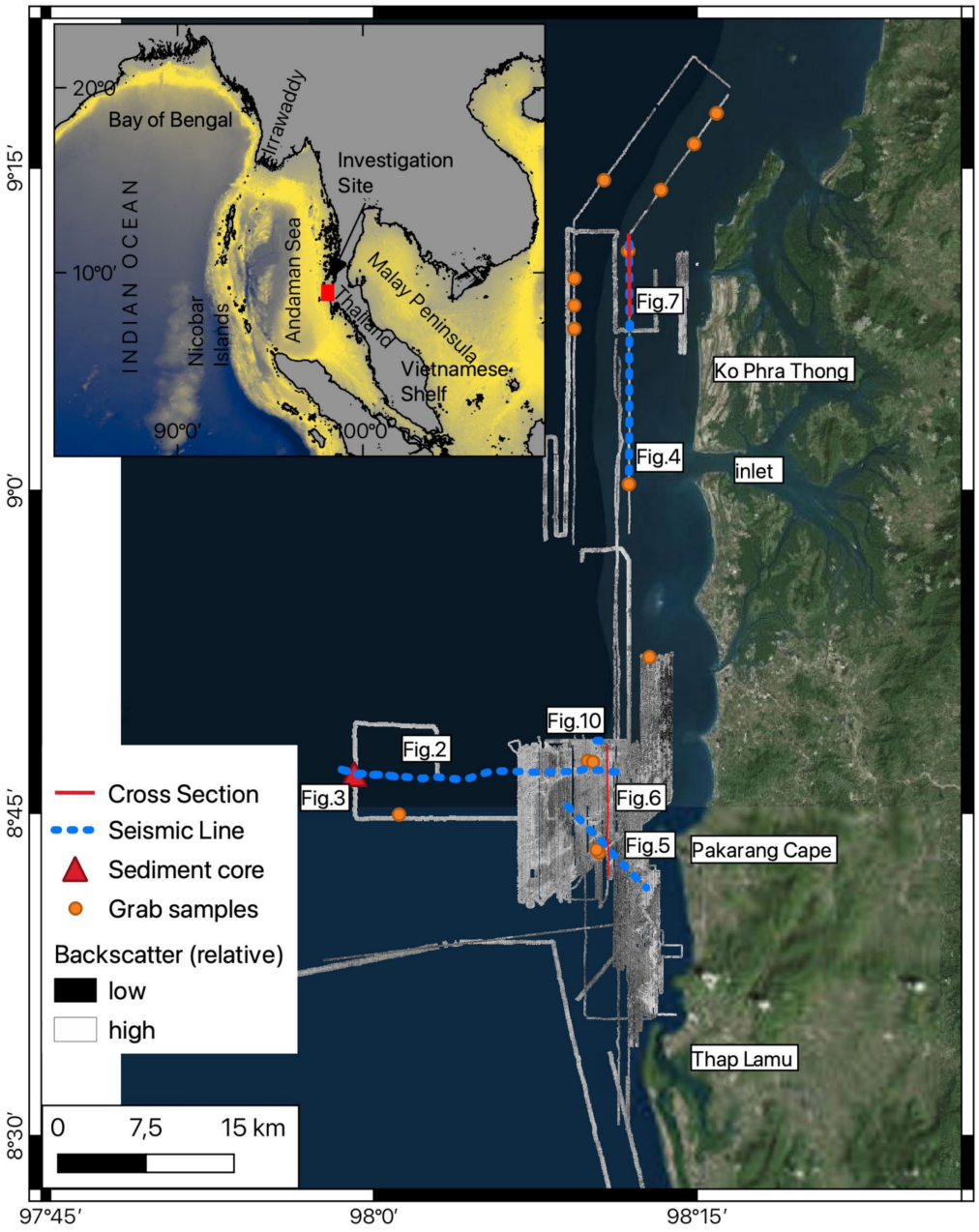

Figure 1. The investigation area offshore Phang Nga Province which is covered by a high resolution side-scan sonar mosaic. The location of core 031207-22 is marked by a red triangle.

The coast is dominated by rocky cliffs alternating with sandy lowlands backed by beach ridges [29]. Offshore of Khao Lak, a fringing reef and an associated drowned paleo-reef have been identified [30]. Previous hydroacoustic mapping (side scan sonar, shallow seismic with different boomer systems) revealed a small-scale channel system incised into a drowned, slightly inclined carbonate platform located approximately 10 m below sea level. The channels serve as sheltered areas in which deposits related to the 2004 Indian Ocean

Tsunami have been preserved [27]. Sediments retrieved by coring and grab sampling could be identified as tsunami deposits by applying geochemical methods [27,31,32], physical proxies (Multi sensor core logger), x-ray images and structural and textural analysis [14]. The influence of the backwash on environmental conditions could be determined in the surface sediments up to 25 km offshore by identifying polycyclic aromatic hydrocarbons, which originate from the terrestrial environment [32]. Net sediment transport from deeper waters into shallower areas was identified by micropalaeontological analyses and the application of foraminiferal transfer functions [33]. Event layers occurring in the sediment cores below the identified 2004 tsunami layers could be related to previous storms and typhoons that were documented for this area with low frequency recurrence [33–35]. Next to typhoon and tsunami deposits, flash flood deposits were identified in the investigation site [35]. From the inner to the mid shelf sand ridges, striking oblique to the coastline, these can be identified down to a water depth of about 30 m. They show a steep NE oriented slope and a gentle SW oriented flank. As the striking of these ridges do not match with the current direction of the tsunami flow observed in IKONOS satellite images, it is assumed that the formation of the ridge system is not related to the 2004 Indian Ocean tsunami [36].

Tin mining activities have a long record in Thailand, starting in 1906 at Phuket Bay and spatially extending to the coastal area of Phang Nga Province. Cassiterite, deposited during sea level lowstand under terrestrial conditions during the glacial periods, is overlain by a thin cover of Holocene marine sediments. These placer deposits had been mined for decades until these activities ceased more than 30 years ago, during the 1980s, due to low tin prices [21].

2.2. Methods

Seismic data was acquired in 2007 onboard RV Chakratong Tongyai, using a Boomer system, comprising a 150–450 J power supply and an 8-element single channel streamer. Seismic data recorded in 2008 and 2010 onboard FS Boolert Pasook was acquired with a low voltage Boomer system (Applied Acoustic Sea C-Boom system) and a 1 element single channel streamer. Data were processed by applying a Butterworth bandpass filter with 400 Hz as the lower and 6000 Hz as the upper cutoff. Subsequently, the line indicating the seafloor reflection was picked, and a low pass filter operating over 50 shot points was applied to reduce swell and wave impact, which unfortunately was partly substantial during data acquisition. Subsequently, a manual gain was applied and three traces were stacked to reduce remaining noise. Two-way travel times were converted to depths using a sound velocity of 1500 m/s for the water column and the upper layers of the seafloor.

Side scan sonar data were recorded in 2007 onboard RV Chakatong Tongyai using a Klein 595 dual frequency side scan sonar with digital data acquisition operating at a frequency of 384 kHz. In 2008, side scan sonar data were recorded onboard FS Boolert Pasook and in 2010 onboard MS Fahsai, using a Benthos 1624 dual frequency side scan sonar, recording with 100 kHz and 400 kHz. The side scan sonar data were slant range corrected and a beam pattern correction was applied. Bathymetric data was collected using a SeaBeam 1185 multibeam system (SeaBeam180 kHz, ELAC Nautic GmbH, Kiel, Germany) in 2008. Data were corrected against sound velocity profiles and further processed using the software mbsystem [37]. However, a failure of the motion compensation significantly reduces data quality and the ability to resolve small vertical differences. Therefore, only data of the central beam is utilized in this study.

In total, 156 sediment samples were retrieved from the seafloor, spread over the 3 cruises using a Van-Veen Type grab sampler. Since the clay and silt content of the samples is generally low, grain size analysis was done by mechanical sieving with 0.25 phi intervals following removal of the components < 0.063 mm. The mode of the grain-size distribution was chosen as a central statistical parameter, as in our case it is not affected by the removal of the fine fraction prior to sieving. A total of 60 short sediment cores were taken, spread over the 3 cruises using a Rumohr-type gravity corer with 7 cm of internal diameter. Core length varied from 0.22 to 2.00 m. In the laboratory, XRF (X-Ray Fluorescence) core scanning was

applied on the split cores to obtain semi-quantitative (measured in counts per second) ratios of 13 elements, including Ti/Ca, following the procedure described in [38] to distinguish between terrestrial and marine deposits. X-ray photos helped to clearly recognize internal sedimentary structures and unconformities. Three subsamples of the sediment cores were dated by ^{14}C in the Leibniz Laboratory for Radiometric Dating and Stable Isotope Research of Kiel University to constrain the time when the shelf was flooded by the postglacial sea level rise.

3. Results

3.1. Mid Shelf

The penetration depth of the used boomer system in up to 60 m water depth varies between 0 to approximately 11 m below the seafloor. Across the shelf, from 30 m to 60 m below sea level (bsl), typically only a thin sediment cover of up to 2 m in thickness overlies the acoustic basement, which frequently forms outcrops built up of hard-rock (granitic) outcrops at the seafloor (see Figure 2).

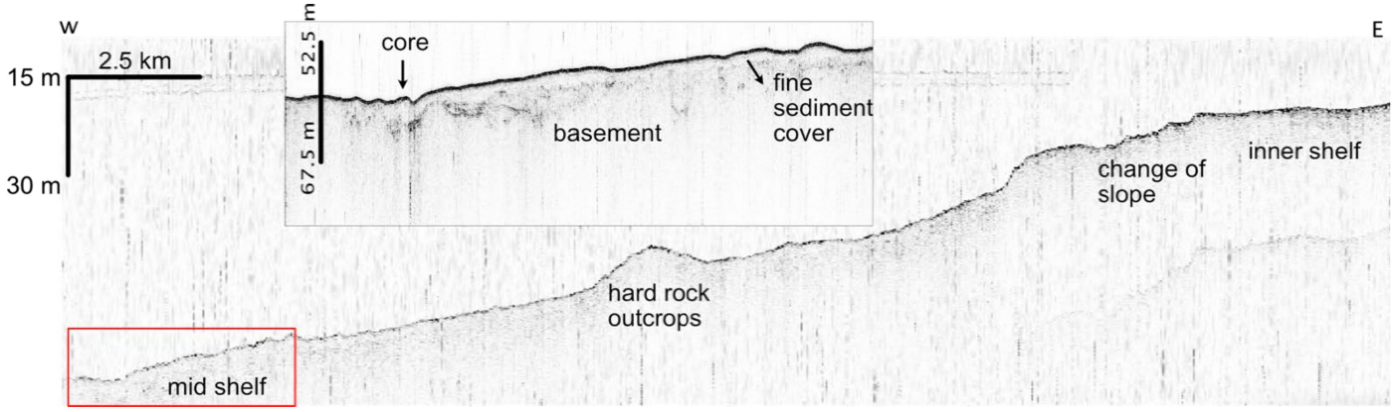

Figure 2. Across-shelf profile showing the flat inner shelf, followed by a change of slope gradient (corresponding to the onset of finer sediment) at 30 m depth, indicated by the scale. The acoustic basement is situated close to the surface of the seafloor (for location of the profile see Figure 1). The thin cover of fine sediments is only visible in the inset, which also shows the location of the sediment core 03120722-02.

Following a break of the slope around 55 m bsl, the observed sediment sequence thickens. Here, the high-amplitude reflector marking the top of the crystalline basement forms steep ridges and incisions. The incisions are filled by faint internally layered and partly acoustically transparent sediment. These infillings have a thickness ranging from 3–4.5 m. However, the thickness is highly variable due to the presence of incisions in the basement. One sediment core from the mid-shelf is discussed in this study (more sediment cores from the investigation site are described in [39]). Core 03120722-02 was retrieved from a water depth of 62 m, targeting an incision in the acoustic basement (Figures 2 and 3). The core has a length of 116 cm and is composed of 2 units. Unit 1 extends from the top to 78 cm and consists mostly of silty sand. Its upper 60 cm are coarsening upwards with an increase of the sand fraction. Shell fragments are scattered throughout the whole unit. A number of event layers, marked by a coarser sediment composition and increased abundance of shells, occur in conjunction with erosional unconformities. Unit 1 is characterized by a gradual increase of the Ti/Ca log-ratio from −2.2 to −1.5. Below 64 cm and a sharp boundary detected in X-Ray images exists, composed of dark silty sand with clay contents of up to 9%. Within unit 2 (below 78 cm core depth), material of plants and pieces of wood are present. At the boundary between unit 1 and 2, the Ti/Ca ratio quickly increases to ~−0.5. Further downcore, it fluctuates between −1.5 and −1. At the very base of the core, the value increases again to −0.5. In total, three wood samples have been retrieved from core depths of 82 and 92 cm. The samples were ^{14}C dated to 12,725–13,427 cal yr BP (Table 1).

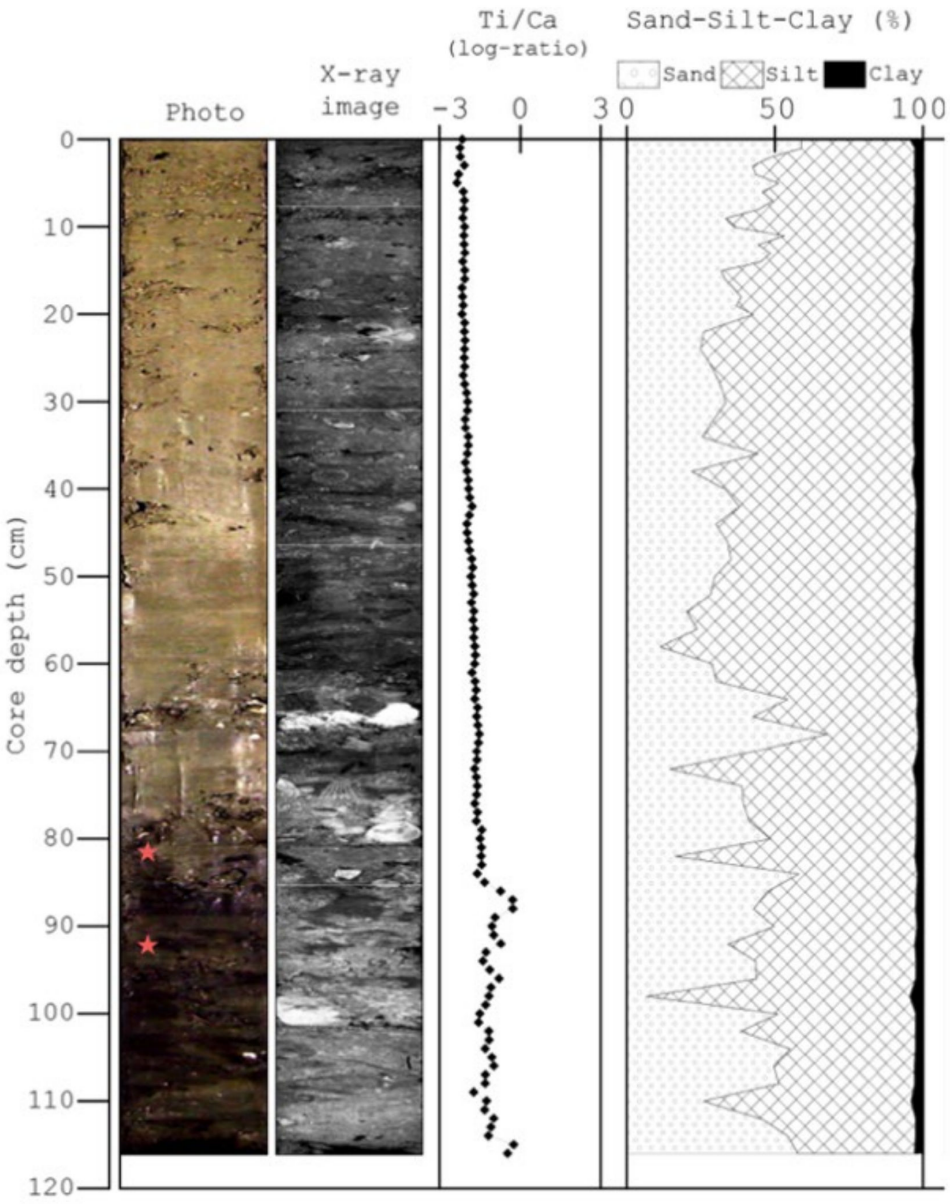

Figure 3. Core 031207-22-02 (62 m water depth). Red stars within the core photo show the depth of sub-samples retrieved for ^{14}C dating. Refer to Figure 1 for core position.

Table 1. Results of ^{14}C dating for material form core 03120722-02. Calibrated ages are calculated with CALIB rev 5.01, database IntCal04 [40].

Laboratory Nr. *	Depth [cm]	Material	δ^{13}C (‰)	^{14}C Age yr BP	Cal Age yr BP: (2 Sigma)
KIA45569	82	wood	-24.60 ± 0.19	$11{,}439 \pm 53$	13,427–13,178
KIA45568	82	wood	-25.85 ± 0.15	$11{,}013 \pm 47$	13,080–12,725
KIA45570	92	wood	-28.64 ± 0.20	$11{,}141 \pm 61$	13,202–12,799

* Leibniz Laboratory for Radiometric Dating and Stable Isotope Research of Kiel University.

3.2. Inner Shelf: Sand Ridges and Associated Morphological Features

Side scan sonar data offshore of Khao Lak were previously interpreted, discerning the facies "fringing reef and adjacent paleoreefs", "sandy inner shelf environment" and "shallow fine-grained sediments (flash flood deposits)" [30]. Here, we focus on the description of sand ridges striking oblique to the coastline in an ENE—SWS direction and associated

elongated patches of finer sediments, characterized by low backscatter intensities, in the inner shelf environment above 28 m bsl.

The sand ridges occur north of Pakarang Cape (Figures 4 and 5). In the available data, none of those ridges have been observed offshore of Thap Lamu and the inlet between Pakarang Cape and the island Ko Phra Thong, where an increasing amount of fine sand accumulates (labelled in Figure 4 as sediment accumulation). Where the ridges have been fully surveyed, their lengths exceed 1 km and can reach up to a maximum of 5.4 km. Offshore of Pakarang Cape, their landward onset is at 17 to 18 m water depth and the ridges fade in water depths of 28 m. This maximum depth coincides with a marked change in the seafloor sediment composition observed in side scan sonar images by a shift to brighter colors (Figure 1), indicating finer-grained sediment. The geomorphology shows a break of the slope in an across-shore direction between the inner and the mid-shelf, seen in the seismic lines (Figure 2). Towards the north, offshore of Ko Phra Thong, only single hydroacoustic profiles cross the sand ridges and therefore their spatial extent across-shelf is unknown. Ridges could only be observed in depths from 20 m to 26 m bsl. However, their dimensions diminish at 26 m water depth, suggesting that the sand ridge system fades out close to this depth.

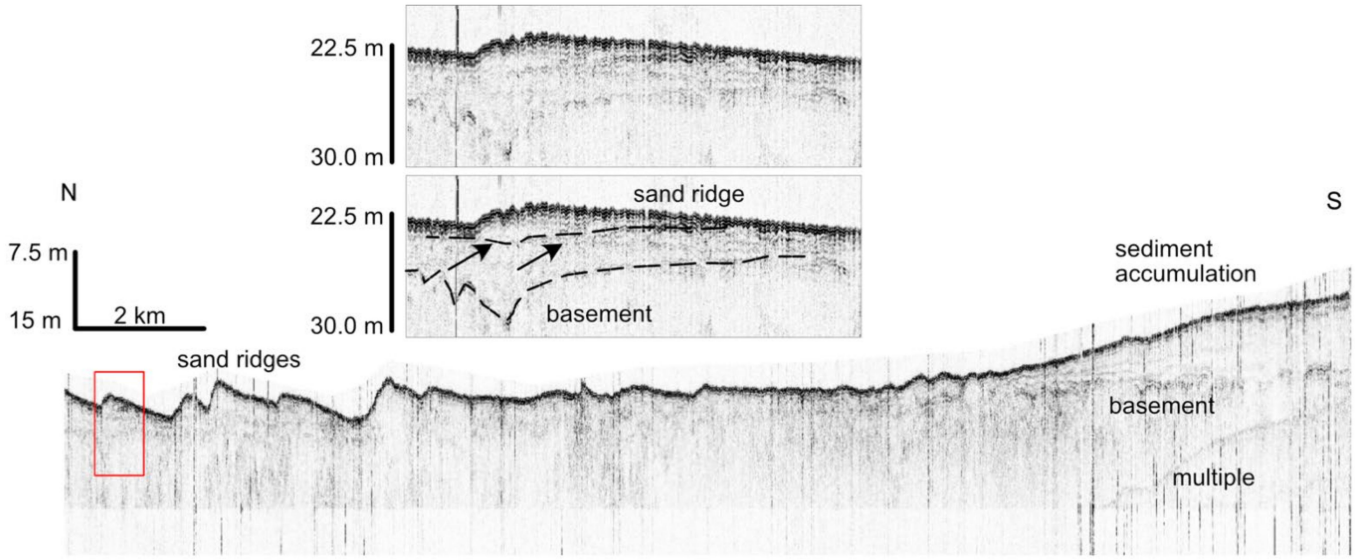

Figure 4. Sand ridges, widespread on the inner shelf, fade towards the inlet between Ko Phra Thong and Pakarang Cape. A reflector is observed at the base of the sand ridges and at the transition to the acoustic basement. The unconformity at the sand ridge base is marked by arrows within the inset. Accumulation of sediment with a transparent appearance in the seismic line is observed offshore of the inlet at Ko Phra Thong. Refer to Figure 1 for position.

The distance between two sand ridge crests varies from almost 4 km offshore of Pakarang Cape (Figure 6) to 600 m at its minimum in the north (Figure 7), with an average of their distance between 1 km and 1.5 km. The strike direction of the ridges varies from 50° to 70°. The bedforms are oblique to the coastline, which is approximately N-S, at approximately the same angle. The sand ridges are asymmetric (Figures 5 and 6), with a steeper seaward (northern) slope and a gentler landward (southern) slope. The seaward slope varies from 0.6° to 1.2°, while the landward slope varies from 0.1° to 0.3°. The height of 23 measured sand ridges varies from 0.6 to 4.2 m, with a mean value of 1.7 m and a standard deviation of 0.9 m. Previously published seismic profiles show an internal stratification in two sand ridges [36]. In most cases, no seismic reflector can be seen at the base of the sand ridges. However, for some ridges, a horizontal unconformity is faintly observed at their base above the acoustic basement (Figures 4 and 5).

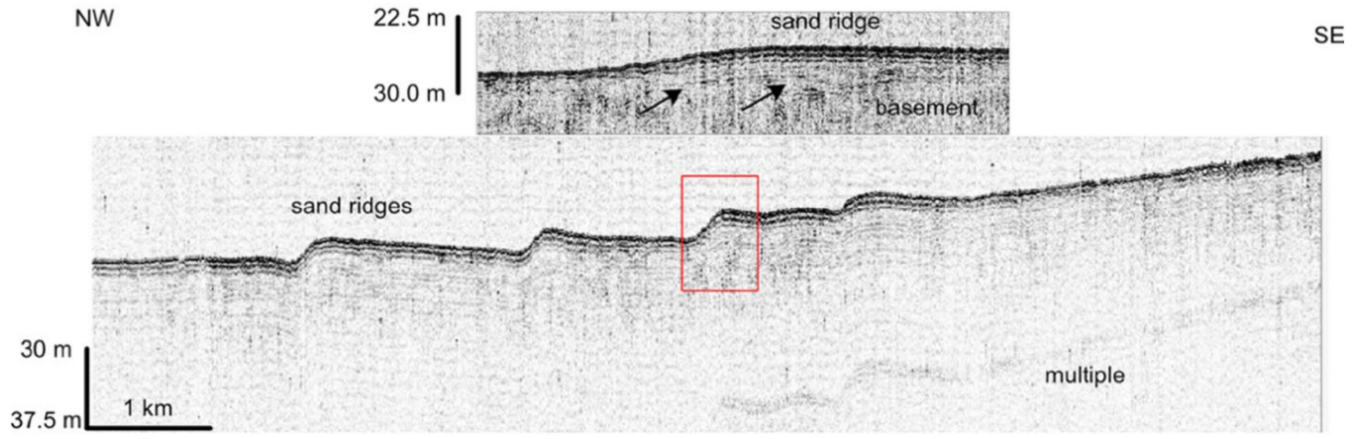

Figure 5. Seismic line south of Pakarang Cape, running perpendicular to the striking of the sand ridges, which are situated closely above the acoustic basement. The unconformity at the ridge base is marked by arrows within the inset. Refer to Figure 1 for position.

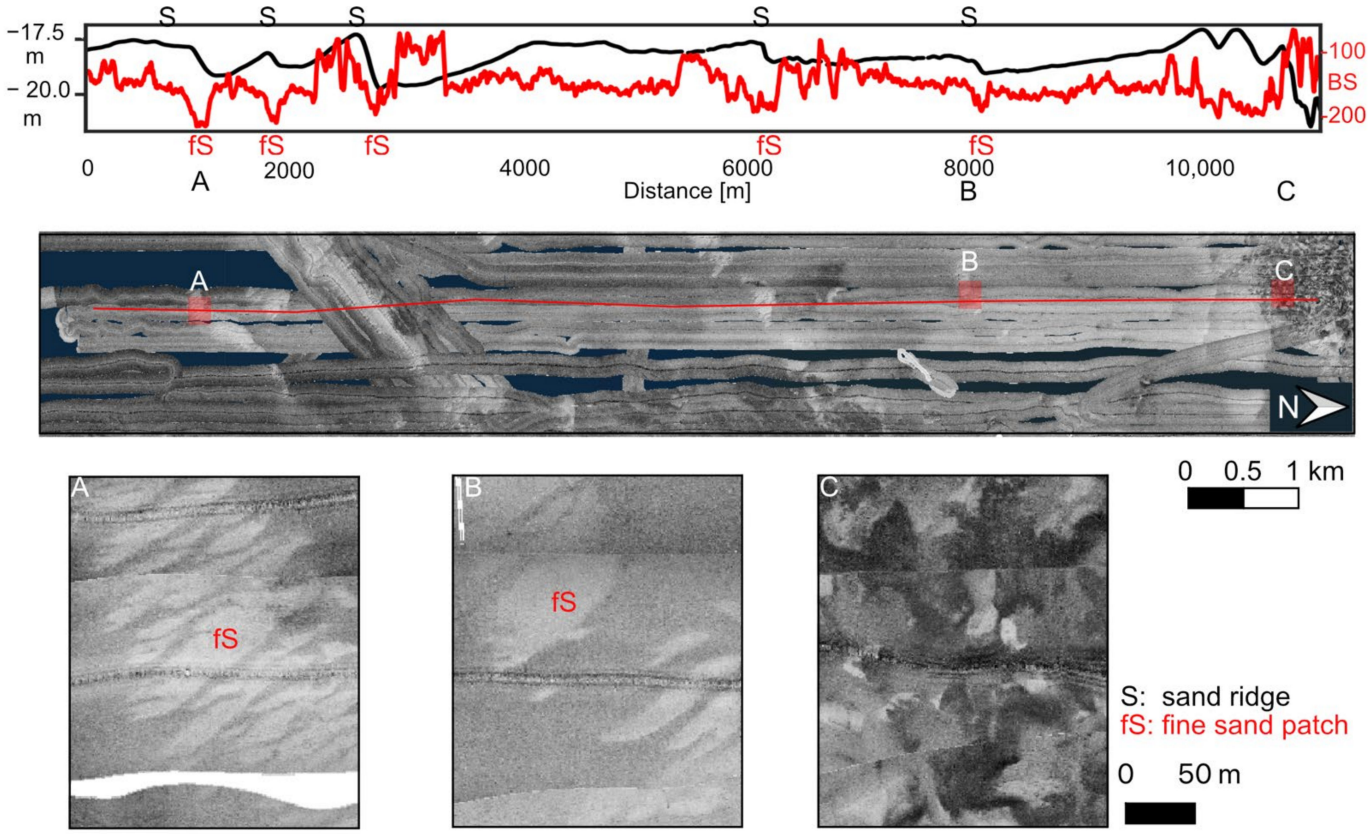

Figure 6. The area of the sand ridges between Thap Lamu and Pakarang Cape observed in the side scan sonar mosaic. The distance between sand ridges as identified in bathymetric cross sections varies from a few hundred meters to approx. 4 km. On the northern, steeper seaward sides of the sand ridges (S), backscatter intensities (BS) decrease (displayed in bright colours) and fine sand forms dune-shaped patterns (fS) parallel to the sand ridge extension (insets A and B). Areas of former tin mining activities in the very north of the profile show a chaotic pattern of high and low backscatter (dark and bright colours) in side scan sonar mosaics (inset C). Please refer to Figure 1 for locations.

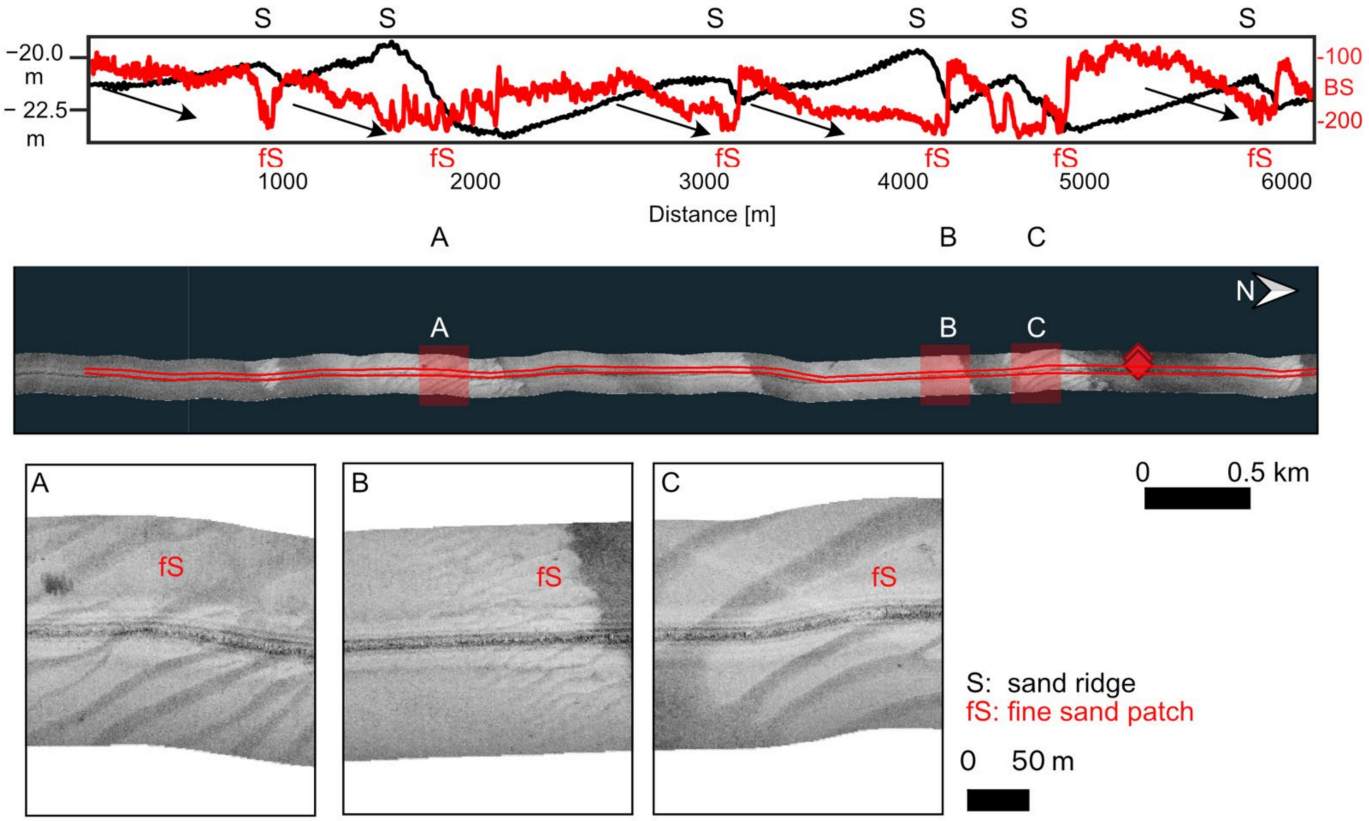

Figure 7. Top: Bathymetry (black lines) and relative backscatter profile (red lines) crossing sand ridges offshore of Ko Phra Thong island in ~20 m bsl. Backscatter intensities (BS) are out of phase with the ridge bathymetry, with intensity decreasing from the trough towards the northern flank (marked by arrows). Similar to the sand ridges (S) between Thap Lamu and Pakarang Cape, the low backscatter patches composed of fine sand (fS) on the northern flank of the ridges form a small dune system, which partly appears very distinct (insets A and C) and partly fuzzy (inset B). Please refer to Figure 1 for location.

The sediments that build up the seaward slope of the sand ridges have a first mode in the fine-to-medium sand fraction (Figure 8), while the landward slope is composed of poorly sorted medium to coarse sand. The seafloor next to the sand ridges is often composed of coarser sediment, which is poorly sorted and includes coral fragments. The first modes are located in the medium to coarse sand fraction (Figure 8).

Fine sand on the seaward side of the ridges forms delicate structures that are observed in side scan sonar mosaics but are not recognized in the seafloor reflection of the seismic profiles. The structures are observed north of Thap Lamu harbor, and their abundance increases north of the inlet between Pakarang Cape and Ko Phra Thong (Figures 6 and 7). They can be of local appearance and are not always observed along the whole length of the sand ridges. The shapes of the patches form a continuum ranging from distinct to fuzzy shapes, with individual widths ranging from a few meters up to 80 m towards continuous, featureless sediment sheets (examples are shown in insets of Figures 6 and 7). The orientation of the features is NNW-SSE, varying from 110° to 135°. The comparison of bathymetric and backscatter data shows that the fine sand forms a dune system on top of the coarser sand substratum, between the crest and trough of the sand ridges. The larger, more distinct features show higher amplitudes and wavelengths, with heights of approximately 0.2 to 0.5 m (Figure 9) and crest-to-crest distances ranging from 20 m to 50 m, while the smaller bedforms have wavelengths of 15 to 25 m. Their heights are less than 0.2 m and thus cannot be reliably resolved within the available bathymetric datasets.

Measured slope values for the larger features vary between 0.2° and 0.7°, with no clear symmetry or asymmetry of the dune flanks.

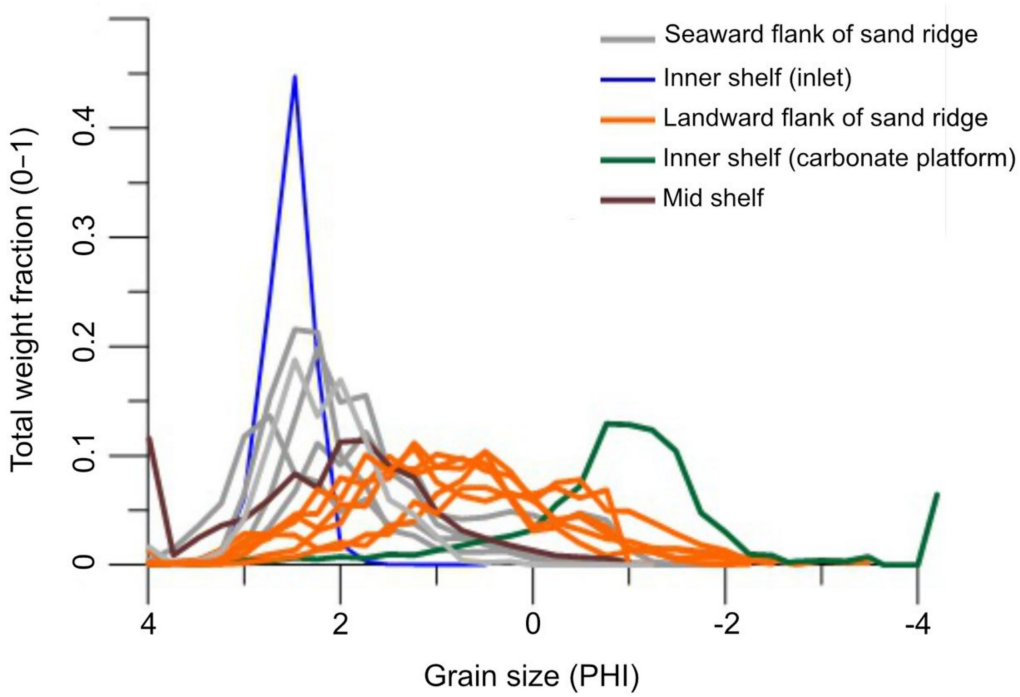

Figure 8. Grain size distribution of selected surface samples. Refer to Figure 1 for position of the samples.

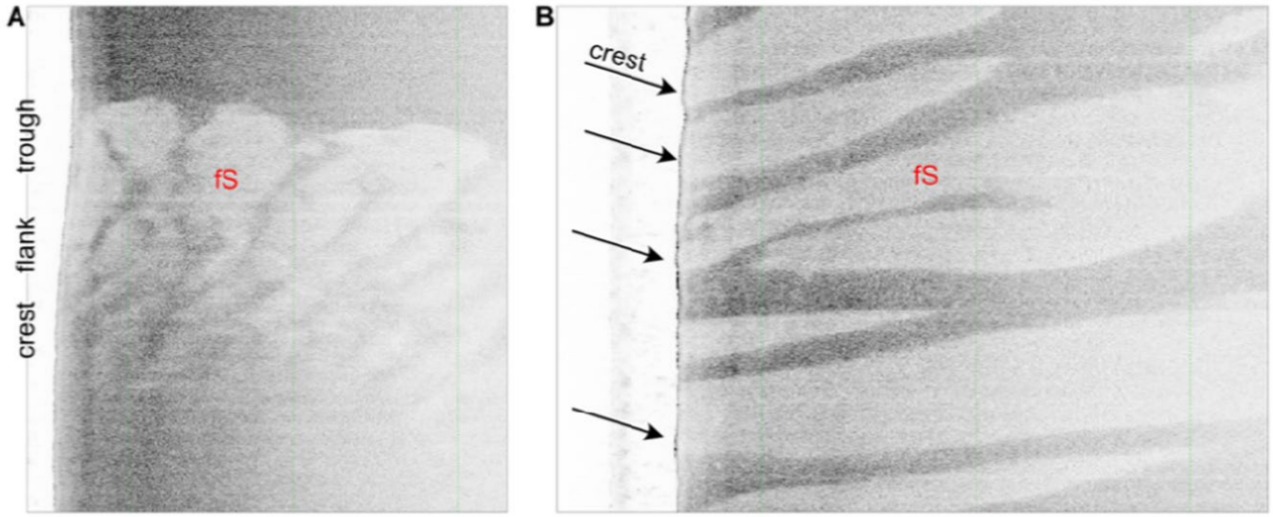

Figure 9. (**A**): Side scan sonar raw data (waterfall picture) from the flank of a sand ridge. No morphological change of the fine sand patches compared to the surrounding seafloor can be seen. (**B**): Distinct patches of fine sand on the seaward side of a ridge are slightly elevated to the surrounding seafloor by about 20 to 50 cm. Spacing of vertical lines is 25 m.

3.3. Remnants of Tin Mining Activities

Despite mining activities stopping more than 25 years before our surveys, remnants of tin mining activities are observed in side scan sonar images and seismic data. Along a seismic profile crossing tin mining holes (Figure 10), up to 8 m deep incisions can be observed. Most holes, however, have a depth of only 2 to 3 m, corresponding to the local thickness of the overlying tin mineral-bearing sediment. Except for the steepest tin mining

holes, no sedimentation subsequent to tin mining activities can be recognized within the vertical resolution limits of the seismic data.

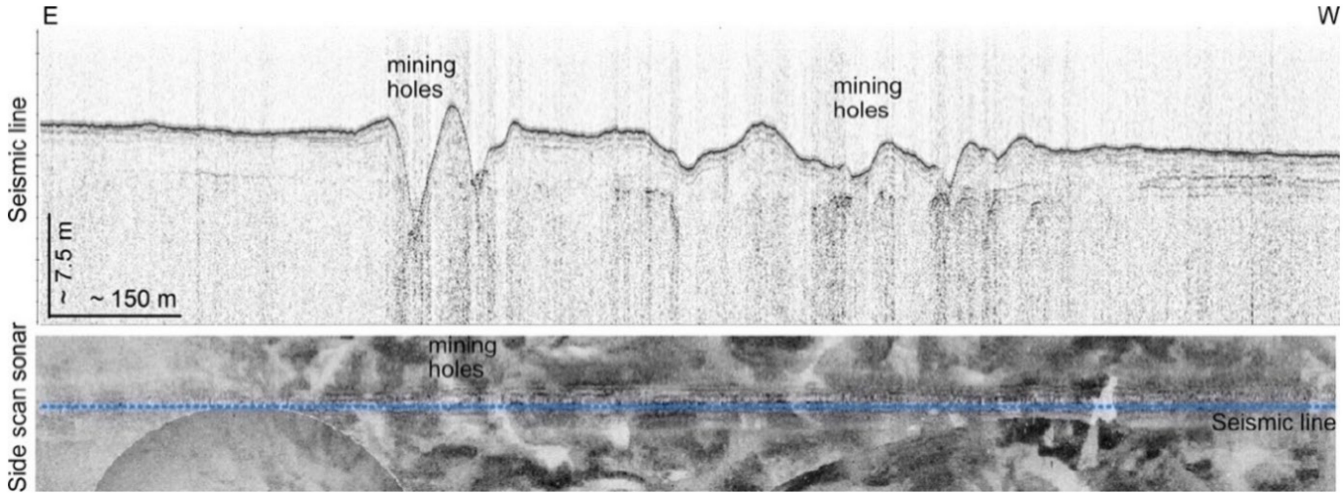

Figure 10. Top: Seismic line and side scan sonar data crossing a former tin mining area, showing holes up to 8 m in depth. Except for the deepest hole, no sedimentation following the end of tin mining activities is observed. Bottom: Side scan sonar data along the seismic line showcases the highly irregular seafloor in the area of former tin mining activities.

4. Discussion

4.1. Holocene Sea Level Rise

The sediment core 03120722-02 from the mid shelf taken at 62 m water depth reveals a change from a terrestrial (lower core unit) to a marine environment (upper core unit). Terrestrial deposits appear only preserved in incisions of the crystalline basement that forms the base of acoustic penetration, indicating a partial reworking of the terrestrial deposits. The transition towards marine conditions is marked by abruptly decreasing Ti/Ca ratios, typical for marine transgression [38] due to the increasing production of $CaCO_3$ by marine species and the decreasing input of Ti deriving from weathered crystalline rocks [41]. The interface between terrestrial and marine deposits, the transgressive surface, is found at the sediment hiatus between core unit 1 and 2 at 78 cm core depth. Wood fragments near this boundary have been dated. The slight age reversal in one wood sample from 82 cm core depth might be caused by sediment reworking during deposition or during the transgression. Therefore, no exact age of the transgression surface is to be expected from the three samples, but a maximum age of the transgression can be constrained.

Deglacial marine flooding of the Andaman Sea shelf passed the present-day water depth of 63 m around 12.7 to 13.4 cal ka BP. This is in agreement with the flooding history of the Sunda Shelf [9,42,43]. The slowly decreasing Ti/Ca ratio towards the top of the sediment core is attributed to the continuing marine transgression and reworking of former terrestrial deposits, but may also be related to the grain size coarsening upward. As no abrupt change of Ti/Ca ratios is observed in the upper 78 cm of the sediment core, we assume that stable conditions were encountered. Further indication for low accumulation rates is provided by the drowned paleo-reef platforms described by [30]. Since sedimentation at sea level maximum positions tends to occur first on the inner shelf before prograding into deeper waters [44], little sedimentation has taken place since the sea level highstand at approx. 6.5 ka BP [9,43]. The low sedimentation rate, also considering a longshore transport of sediments, and the limited availability of mobile sediment, is further reflected in the presence of the unfilled tin mining holes. Within seismic data with a vertical resolution of approximately 10 cm, no re-filling is observed in the majority of the holes, with the exception of the deepest hole. Since sedimentation pattern and sediment dynamics are unlikely to change across the comparatively small tin mining field, we assume that sedimentation in these holes takes place by slumping, as observed in other offshore mining areas [45]. The

stability of these forms is similar to bedforms on other sediment-starved shelves such as parts of the North Sea [8,46,47] or the Baltic Sea [48].

4.2. Bedforms on the Inner Shelf

Sand ridges are widespread on continental shelves, and are well described from the shelf of the eastern Atlantic and from the Dutch part of the North Sea [49,50]. They are formed by tidal currents or by wind/storm generated currents and can persist for millennia [51]. Both active and relict forms are known [50]. The morphology-grain size relationship can be used to differentiate between tidal- and storm-generated sand ridges [50]. Those formed by tidal currents typically show the finest sediment in the ridge troughs. Conversely, ridges generated by wind-induced currents have an out-of-phase relationship between morphology and grain size, with the coarser sediment on the landward side and the finest sediment on the seaward side [52,53]. While grab samples across the ridge crests in the investigation site are not sufficiently dense to assess this grain size trend, the backscatter strength in the side scan mosaic is used, following an approach described in [54], to assess the relative grain size changes across the sand ridges (Figures 6 and 7). The backscatter strength shows an out-of-phase grain size relationship. Therefore, the sand ridges offshore Khao Lak are likely to have been formed by storm/wind generated currents and not by the peak tidal flow, although tidal residual currents cause or contribute to the local south-north directed sediment transport [23,25]. This is well in agreement with the observed sand ridge dimensions, as tidal sand ridges tend to be an order of magnitude larger (up to 43 m), steeper (up to 6° slope) and wider (up to 70 km) compared to the sand ridge system offshore of Khao Lak. However, in some instances it was described that tidal- and storm-generated sand ridges can be of similar dimensions [55]. These smaller sand ridges, e.g., those observed on the Dutch banks, are still actively shaped and are migrating [49,56].

An important question is whether the sand ridges are actively being shaped or represent a relict morphology [57]. An indication to consider the sand ridges as relict bedforms is the presence of a coral platform landwards of the sand ridges [30]. The only recent background deposits that have been found on these platforms (not accounting for tsunami and storm deposits) are flash flood deposits composed of fine silt and clay, showing very little annual dynamism [35]. It appears unlikely that these silty and unconsolidated sediments would accumulate close to the shoreline, while the medium to coarse sand comprising the sand ridge material is transported. This would require different hydrodynamic regimes in direct vicinity [58], and thus shows that the ridges have at least not been active in the period of our surveys from 2008–2010. The measured height of the sand ridges, all lower than 4.5 m and typically less than 2.5 m high, agree with globally observed relict features [59]. Active wind- and storm-generated ridges typically exceed these heights.

Different morphologies of non-tidal sand ridges have been proposed, termed shoreface ridges, nearshore ridges and offshore ridges [52,60]. These three morphologies separate the different evolutionary stages of individual sand ridges [59]. Due to their marked asymmetry, with the seaward slope being 3 to 4 times steeper compared to the landward slope, the lack of branches and their occurrence in water depths below 15 m, the ridge system offshore of Khao Lak is classified as an offshore ridge system. The observed dune system, with elongated patches of low backscatter in the troughs on the seaward side of the sand ridges, agrees with the interpretation of offshore ridges. On the seaward side, finer sediments (frequently fine sand) [61], partly forming small dunes or megaripples [52], are present. The changing morphological characteristics from shoreface connected ridges to nearshore and offshore ridges is explained with a) the decreasing energy and frequency of storm impact and b) an increasing importance of storm mean flow currents due to the Holocene sea level rise [52].

The investigation area is a Holocene tropical far field site, reaching a maximum sea level highstand of +2.5 m at around 6.5 ky BP [9,43,62]. Therefore, it appears likely that the sand ridge system originally formed during the transgression prior to 6.5 ky BP. Applying

the sea level curve for the Vietnamese shelf [43] to the Andaman Sea, which at least is not ruled out by the available sea level curve constraint shown in this study, and given the present minimum observed depth of the sand ridge system of 17 to 18 m water depth, the sand ridge system development started at ~9.0 ka BP on top of a ravinement surface during a transgressive period [51]. Subsequently, the ridges quickly shifted to greater water depths following the rapid sea level rise between 9.0 ka BP and 8.2 ka BP.

To what extent the sand ridge field is still active during the rare, strong storm events [34] hitting this part of the Thai coastline cannot be resolved with our data. In any case, based on the available grain size distributions (Figure 8), it may be presumed that sediment winnowing and hiding still takes place over the sand ridge system [50], moving fine particles to the sheltered, seaward environment and leaving a poorly sorted sediment distribution on the landward side of the sand ridges. The fine sand patches are forming a small dune system that developed on the seaward side of the sand ridges. Similar patterns are described by [63] and [53]. While certainly underestimated due to the limited resolution of the low-quality bathymetric data, the dune height to wavelength (H/L) relationship of these dune systems is situated clearly beneath the global equilibrium line [64]. Deviations from the global equilibrium line indicate a partial reworking and/or a lack of sediment available for dune formation [65]. This is in agreement with the general lack of mobile deposits on the Andaman shelf that is readily apparent from seismic data (e.g., Figure 4). Principally, the dune system on the seaward flanks of the sand ridges has to be formed by WSW-ENE directed currents, which is in contrast to the S-N net longshore current and sediment transport in the area. Given the presence of strong winds, especially during the southwest monsoon lasting from May to September (while our surveys took place in January and February), it may be speculated that the dune system is active during that period. Movement of sandwaves in 20 m depth due to monsoon-driven currents is known from the Australian shelves [66,67].

5. Conclusions

A first data point indicates a similar transgression pattern of the Andaman Sea and the Sunda Shelf, with the approx. 63 m present day water depth transgressed around 12.8 to 13.4 cal ka BP at maximum. Later on, during sea level transgression, sediment starved conditions prevailed and a series of sand ridges developed. At present, these sand ridges are likely to be inactive, while a smaller dune system has developed on their seaward flanks. The apparent lack of mobile sediments indicates that the effects of coastal retreat due to the predicted rising sea-level cannot be counteracted by additional sediment supply from the inner shelf. Additionally, anthropogenic impacts on the shelf such as the extraction of mineral resources will leave a disturbed shelf environment for decades, as there is not sufficient mobile sediment available to refill the mining holes.

Author Contributions: Conceptualization, K.S. and P.F.; methodology, P.F., K.S., D.S.-S., S.K.; formal analysis, P.F., K.S., D.S.-S.; investigation, K.S., P.F., D.S.-S.; resources, K.S., S.K., P.F.; data curation, K.S.; writing—original draft preparation, P.F., K.S.; writing—review and editing, D.S.-S., S.K.; visualization, P.F.; project administration, K.S.; funding acquisition, K.S., S.K. All authors have read and agreed to the published version of the manuscript.

Funding: This research was funded by Deutsche Forschungsgemeinschaft (DFG) grant No. SCHW 572/11-1 and National Research Council of Thailand (NRCT).

Institutional Review Board Statement: Not applicable.

Informed Consent Statement: Not applicable.

Data Availability Statement: The side scan sonar mosaics are available at https://doi.org/10.5281/zenodo.5749357, doi:10.5281/zenodo.5749357, accessed on 24 January 2022.

Acknowledgments: We would like to thank Phuket Marine Biological Center (PMBC) for supporting us with ship time of RV Chakratong Tongyai and RV Boonlert Pasook and the captains and crews for

their support during the surveys in 2007, 2008 and 2010. Thanks as well to 3 anonymous reviewers for their valuable comments to the manuscript.

Conflicts of Interest: The authors declare no conflict of interest. The funders had no role in the design of the study; in the collection, analyses, or interpretation of data; in the writing of the manuscript, or in the decision to publish the result.

References

1. Chiocci, F.L.; Chivas, A. An overview of the continental shelves of the world. *Geol. Soc. Lond. Mem.* **2014**, *41*, 1–5. [CrossRef]
2. Green, M.O.; Coco, G. Review of wave-driven sediment resuspension and transport in estuaries. *Rev. Geophys.* **2014**, *52*, 77–117. [CrossRef]
3. Schwarzer, K.; Diesing, M.; Larson, M.; Niedermeyer, R.-O.; Schumacher, W.; Furmanczyk, K. Coastline evolution at different time scales—Examples from the Pomeranian Bight, southern Baltic Sea. *Mar. Geol.* **2003**, *194*, 79–101. [CrossRef]
4. Einsele, G. Sedimentary basins. In *Evolution, Facies, and Sediment Budget*; Springer: Berlin, Germany, 2001.
5. Swift, D.J.P.; Thorne, J.A. Sedimentation on continental margins, I: A general model for shelf sedimentation. In *Shelf Sand and Sandstone Bodies*; Swift, D.J.P., Oertel, G.F., Tillman, R.W., Thorne, J.A., Eds.; Blackwell Scientific Publications: Oxford, UK; London, UK; Edinburgh, UK; Cambridge, MA, USA; Carlton, Australia, 1992; pp. 1–31. [CrossRef]
6. Emery, K.O.; Uchupi, E. Western North Atlantic Ocean. Memoir 17, American Association of Petroleum Geologist, Tulsa, Oklahoma. 532 pp., 330 figs. Price U.S. $30.00. *Geol. Mag.* **1974**, *111*, 189. [CrossRef]
7. Milliman, J.D.; Syvitski, J.P.M. Geomorphic/Tectonic Control of Sediment Discharge to the Ocean: The Importance of Small Mountainous Rivers. *J. Geol.* **1992**, *100*, 525–544. [CrossRef]
8. Diesing, M.; Kubicki, A.; Winter, C.; Schwarzer, K. Decadal scale stability of sorted bedforms, German Bight, southeastern North Sea. *Cont. Shelf Res.* **2006**, *26*, 902–916. [CrossRef]
9. Hanebuth, T.; Stattegger, K.; Grootes, P.M. Rapid Flooding of the Sunda Shelf: A Late-Glacial Sea-Level Record. *Science* **2000**, *288*, 1033–1035. [CrossRef]
10. Peltier, W.R.; Fairbanks, R.G. Global glacial ice volume and Last Glacial Maximum duration from an extended Barbados sea level record. *Quat. Sci. Rev.* **2006**, *25*, 3322–3337. [CrossRef]
11. Streif, H. Sedimentary record of Pleistocene and Holocene marine inundations along the North Sea coast of Lower Saxony, Germany. *Quat. Int.* **2004**, *112*, 3–28. [CrossRef]
12. Dangendorf, S.; Hay, C.; Calafat, F.M.; Marcos, M.; Piecuch, C.G.; Berk, K.; Jensen, J. Persistent acceleration in global sea-level rise since the 1960s. *Nat. Clim. Chang.* **2019**, *9*, 705–710. [CrossRef]
13. Vital, H.; Stattegger, K.; Amaro, V.E.; Schwarzer, K.; Frazão, E.P.; Tabosa, W.F.; Silveira, I.M. A modern high-energy si-liciclastic-carbonate platform: Continental shelf adjacent to northern Rio Grande do Norte State, northeastern Brazil. *J. Sediment. Res.* **2008**, *90*, 175–188.
14. Schwarzer, K. Geophysical prospection and sedimentological characteristics of subaquatic tsunami deposits. In *Geological Records of Tsunamis and Other Extreme Waves*; Engel, M., Pilarczyk, J., May, S.M., Brill, D., Garret, E., Eds.; Elsevier: Amsterdam, The Netherlands, 2020; pp. 115–142.
15. Feldens, P.; Diesing, M.; Schwarzer, K.; Heinrich, C.; Schlenz, B. Occurrence of flow parallel and flow transverse bedforms in Fehmarn Belt (SW Baltic Sea) related to the local palaeomorphology. *Geomorphology* **2015**, *231*, 53–62. [CrossRef]
16. Kleinhans, M.G.; Wilbers, A.W.E.; De Swaaf, A.; Van Den Berg, J.H. Sediment Supply-Limited Bedforms in Sand-Gravel Bed Rivers. *J. Sediment. Res.* **2002**, *72*, 629–640. [CrossRef]
17. Kamesh Raju, K.A.; Ramprasad, T.; Rao, P.S.; Ramalingeswara Rao, B.; Varghese, J. New insights into the tectonic evolution of the Andaman basin, northeast Indian Ocean. *Earth Planet. Sci. Lett.* **2004**, *221*, 145–162. [CrossRef]
18. Liu, J.P.; Kuehl, S.A.; Pierce, A.C.; Williams, J.; Blair, N.E.; Harris, C.; Aung, D.W.; Aye, Y.Y. Fate of Ayeyarwady and Thanlwin Rivers Sediments in the Andaman Sea and Bay of Bengal. *Mar. Geol.* **2020**, *423*, 106137. [CrossRef]
19. Ramaswamy, V.; Rao, P.S.; Rao, K.H.; Thwin, S.; Rao, N.S.; Raiker, V. Tidal influence on suspended sediment distribution and dispersal in the northern Andaman Sea and Gulf of Martaban. *Mar. Geol.* **2004**, *208*, 33–42. [CrossRef]
20. Rao, P.S.; Ramaswamy, V.; Thwin, S. Sediment texture, distribution and transport on the Ayeyarwady continental shelf, Andaman Sea. *Mar. Geol.* **2005**, *216*, 239–247. [CrossRef]
21. Usiriprisan, C.; Chiemchindaratana, S.; Shoosuwan, Y.S. *Chatrapakpong. Offshore Exploration for Tin and Heavy Minerals in the Andaman Sea*; Department of Mineral Resources: Bangkok, Thailand; UNDP: New York, NY, USA, 1987; p. 224.
22. Bunopas, S.; Piyasin, S.; Nutasari, N. *Toraniwitayapratetthai (Geology of Thailand)*; Department of Mineral Resources: Bangkok, Thailand, 2001. (In Thai)
23. Geronimo, I.D.; Choowong, M.; Phantuwongraj, S. Geomorphology and Superficial Bottom Sediments of Khao Lak Coastal Area (SW Thailand). *Pol. J. Environ. Stud.* **2009**, *18*, 111–121.
24. Schwab, J.M.; Krastel, S.; Grun, M.; Gross, F.; Pananont, P.; Jintasaeranee, P.; Bunsomboonsakul, S.; Weinrebe, W.; Winkelmann, D. Submarine mass wasting and associated tsunami risk offshore western Thailand, Andaman Sea, Indian Ocean. *Nat. Hazards Earth Syst. Sci.* **2012**, *12*, 2609–2630. [CrossRef]
25. Dheeradilok, P. Quaternary coastal morphology and deposition in Thailand. *Quat. Int.* **1995**, *26*, 49–54. [CrossRef]

26. Murty, T.S.; Flather, R.A. Impact of storm surges in the Bay of Bengal. *J. Coast. Res.* **1994**, *12*, 149–161.
27. Sakuna, D.; Szczuciński, W.; Feldens, P.; Schwarzer, K.; Khokiattiwong, S. Sedimentary deposits left by the 2004 Indian Ocean tsunami on the inner continental shelf offshore of Khao Lak, Andaman Sea (Thailand). *Earth Planets Space* **2012**, *64*, 931–943. [CrossRef]
28. Thampanya, U.; Vermaat, J.; Sinsakul, S.; Panapitukkul, N. Coastal erosion and mangrove progradation of Southern Thailand. *Estuar. Coast. Shelf Sci.* **2006**, *68*, 75–85. [CrossRef]
29. Brill, D.; Jankaew, K.; Neubauer, N.-P.; Kelletat, D.; Scheffers, A.; Vött, A.; Brückner, H. Holocene coastal evolution of southwest Thailand—Implications for the site-specific preservation of palaeotsunami deposits. *Z. Geomorphol.* **2014**, *58*, 273–303. [CrossRef]
30. Feldens, P.; Schwarzer, K.; Sakuna, D.; Szczuciński, W.; Sompongchaiyakul, P. Sediment distribution on the inner continental shelf off Khao Lak (Thailand) after the 2004 Indian Ocean tsunami. *Earth Planets Space* **2012**, *64*, 875–887. [CrossRef]
31. Pongpiachan, S.; Tipmanee, D.; Deelaman, W.; Muprasit, J.; Feldens, P.; Schwarzer, K. Risk assessment of the presence of polycyclic aromatic hydrocarbons (PAHs) in coastal areas of Thailand affected by the 2004 tsunami. *Mar. Pollut. Bull.* **2013**, *76*, 370–378. [CrossRef]
32. Tipmanee, D.; Deelaman, W.; Pongpiachan, S.; Schwarzer, K.; Sompongchaiyakul, P. Using Polycyclic Aromatic Hydrocarbons (PAHs) as a chemical proxy to indicate Tsunami 2004 backwash in Khao Lak coastal area, Thailand. *Nat. Hazards Earth Syst. Sci.* **2012**, *12*, 1441–1451. [CrossRef]
33. Milker, Y.; Wilken, M.; Schumann, J.; Sakuna, D.; Feldens, P.; Schwarzer, K.; Schmiedl, G. Sediment transport on the inner shelf off Khao Lak (Andaman Sea, Thailand) during the 2004 Indian Ocean tsunami and former storm events: Evidence from foraminiferal transfer functions. *Nat. Hazards Earth Syst. Sci.* **2013**, *13*, 3113–3128. [CrossRef]
34. Phantuwongraj, S.; Choowong, M. Tsunamis versus storm deposits from Thailand. *Nat. Hazards* **2012**, *63*, 31–50. [CrossRef]
35. Sakuna-Schwartz, D.; Feldens, P.; Schwarzer, K.; Khokiattiwong, S.; Stattegger, K. Internal structure of event layers preserved on the Andaman Sea continental shelf, Thailand: Tsunami vs. storm and flash-flood deposits. *Nat. Hazards Earth Syst. Sci.* **2015**, *15*, 1181–1199. [CrossRef]
36. Feldens, P.; Sakuna, D.; Schwarzer, K.; Somgpongchaiyakul, P. Shallow water sediment structures in a tsunami-affected area (Pakarang Cape, Thailand). *Coastline Rep.* **2010**, *16*, 15–25.
37. Caress, D.W.; Chayes, D.N. Improved processing of Hydrosweep DS multibeam data on the R/V Maurice Ewing. *Mar. Geophys. Res.* **1996**, *18*, 631–650. [CrossRef]
38. Tjallingii, R.; Stattegger, K.; Wetzel, A.; Van Phach, P. Infilling and flooding of the Mekong River incised valley during deglacial sea-level rise. *Quat. Sci. Rev.* **2010**, *29*, 1432–1444. [CrossRef]
39. Sakuna-Schwartz, D. Sedimentation characteristics on the Andaman shelf, Thailand: Unraveling extreme events. *Inst. Geosci. Kiel.* **2013**, *83*, 1–68.
40. Reimer, P.J. Intcal04: Terestrial radiocarbon age calibration, 0–26 cal kyr BP. *Radiocarbon* **2004**, *46*, 1029–1058.
41. Calvert, S.E.; Pedersen, T.F. Chapter Fourteen Elemental Proxies for Palaeoclimatic and Palaeoceanographic Variability in Marine Sediments: Interpretation and Application. *Dev. Mar. Geol.* **2007**, *1*, 567–644.
42. Schimanski, A.; Stattegger, K. Deglacial and Holocene evolution of the Vietnam shelf: Stratigraphy, sediments and sea-level change. *Mar. Geol.* **2005**, *214*, 365–387. [CrossRef]
43. Tjallingii, R.; Stattegger, K.; Stocchi, P.; Saito, Y.; Wetzel, A. Rapid flooding of the southern Vietnam shelf during the early to mid-Holocene. *J. Quat. Sci.* **2014**, *29*, 581–588. [CrossRef]
44. Gao, S.; Collins, M.B. Holocene sedimentary systems on continental shelves. *Mar. Geol.* **2014**, *352*, 268–294. [CrossRef]
45. Michaelis, R.; Hass, H.C.; Mielck, F.; Papenmeier, S.; Sander, L.; Ebbe, B.; Gutow, L.; Wiltshire, K.H. Hard-substrate habitats in the German Bight (South-Eastern North Sea) observed using drift videos. *J. Sea Res.* **2019**, *144*, 78–84. [CrossRef]
46. Diesing, M.; Schwarzer, K. Identification of submarine hard-bottom substrates in the German North Sea and Baltic Sea EEZ with high-resolution acoustic seafloor imaging. In *Progress in Marine Conservation in Europe*; Springer Science and Business Media LLC: Berlin/Heidelberg, Germany, 2006; pp. 111–125.
47. Zeiler, M.; Schulz-Ohlberg, J.; Figge, K. Mobile sand deposits and shoreface sediment dynamics in the inner German Bight (North Sea). *Mar. Geol.* **2000**, *170*, 363–380. [CrossRef]
48. Diesing, M.; Schwarzer, K.; Zeiler, M.; Klein, H. Comparison of marine sediment extraction sites by means of shoreface zona-tion. *J. Coast. Res.* **2006**, *SI39*, 783–788.
49. Van de Meene, J.W.H.; van Rijn, L.C. The shoreface-connected ridges along the central Dutch coast—Part 2: Morphological modelling. *Cont. Shelf Res.* **2000**, *20*, 2325–2345. [CrossRef]
50. Holland, K.T.; Elmore, P.A. A review of heterogeneous sediments in coastal environments. *Earth-Sci. Rev.* **2008**, *89*, 116–134. [CrossRef]
51. Snedden, J.W.; Dalrymple, R.W. Modern shelf sand ridges: From historical perspective to a unified hydrodynamic and evo-lutionary model. *Quat. Int.* **1999**, *112*, 3–28.
52. Swift, D.J.P.; Field, M.E. Evolution of a classic sand ridge field: Maryland sector, North American inner shelf. *Sedimentology* **1981**, *28*, 461–482. [CrossRef]
53. Goff, J.A.; Swift, D.J.P.; Duncan, C.S.; Mayer, L.A.; Hughes-Clarke, J. High-resolution swath sonar investigation of sand ridge, dune and ribbon morphology in the offshore environment of the New Jersey margin. *Mar. Geol.* **1999**, *161*, 307–337. [CrossRef]

54. Goff, J.A.; Olson, H.C.; Duncan, C.S. Correlation of side-scan backscatter intensity with grain-size distribution of shelf sediments, New Jersey margin. *Geo-Mar. Lett.* **2000**, *20*, 43–49. [CrossRef]
55. Kenyon, N.H.; Belderson, R.H.; Stride, A.H.; Johnson, M.A. Offshore tidal sand-banks as indicators of net sand transport and as potential deposits. In *Holocene Marine Sedimentation in the North Sea Basin*; Wiley: Hoboken, NJ, USA, 1981; pp. 257–268.
56. Van de Meene, J.W.H.; van Rijn, L.C. The shoreface-connected ridges along the central Dutch coast—Part 1: Field observations. *Cont. Shelf Res.* **2000**, *20*, 2295–2323. [CrossRef]
57. Dyer, K.R.; Huntley, D.A. The origin, classification and modelling of sand banks and ridges. *Cont. Shelf Res.* **1999**, *19*, 1285–1330. [CrossRef]
58. Belderson, R.H. Offshore tidal and non-tidal sand ridges and sheets: Differences in morphology and hydrodynamic setting. *Holocene Mar. Sediment. North Sea Basin* **1986**, *5*, 257–268.
59. Amos, C.L.; King, E.L. Bedforms of the Canadian eastern seaboard: A comparison with global occurrences. *Mar. Geol.* **1984**, *57*, 167–208. [CrossRef]
60. Pendleton, E.A.; Brothers, L.L.; Thieler, E.R.; Sweeney, E.M. Sand ridge morphology and bedform migration patterns derived from bathymetry and backscatter on the inner-continental shelf offshore of Assateague Island, USA. *Cont. Shelf Res.* **2017**, *144*, 80–97. [CrossRef]
61. Swift, D.J.P.; Parker, G.; Lanfredi, N.W.; Perillo, G.; Figge, K. Shoreface-connected sand ridges on American and European shelves: A comparison. *Estuar. Coast. Mar. Sci.* **1978**, *7*, 257–273. [CrossRef]
62. Scheffers, A.; Brill, D.; Kelletat, D.; Brückner, H.; Scheffers, S.; Fox, K. Holocene sea levels along the Andaman Sea coast of Thailand. *Holocene* **2012**, *22*, 1169–1180. [CrossRef]
63. Durán, R.; Guillén, J.; Rivera, J.; Muñoz, A.; Lobo, F.J.; Fernández-Salas, L.M.; Acosta, J. Subaqueous dunes over sand ridges on the Murcia outer shelf. In *Atlas of Bedforms in the Western Mediterranean*; Springer: Singapore, 2017; pp. 187–192.
64. Flemming, B.W. Zur klassifikation subaquatischer, strömungstransversaler Transportkörper. *Boch. Geol. Und Geotech. Arb.* **1988**, *29*, 44–47.
65. Tuijnder, A.P.; Ribberink, J.S.; Hulscher, S.J.M.H. An experimental study into the geometry of supply-limited dunes. *Sedimentology* **2009**, *56*, 1713–1727. [CrossRef]
66. Harris, P.T. Reversal of subtidal dune asymmetries caused by seasonally reversing wind-driven currents in Torres Strait, northeastern Australia. *Cont. Shelf Res.* **1991**, *11*, 655–662. [CrossRef]
67. Harris, P.T. Sandwave movement under tidal and wind-driven currents in a shallow marine environment: Adolphus Channel, northeastern Australia. *Cont. Shelf Res.* **1989**, *9*, 981–1002. [CrossRef]